Systematic calculations of low-lying states in odd-*A* nuclei within the nucleon pair approximation

L. Y. Jia,[1,2,*] H. Zhang,[1,3] and Y. M. Zhao[1,4,5,†]

[1]*Department of Physics, Shanghai Jiao Tong University, Shanghai 200240, People's Republic of China*

[2]*Department of Electrical Engineering, Shanghai Jiao Tong University, Shanghai 200240, People's Republic of China*

[3]*Department of Biology, Shanghai Jiao Tong University, Shanghai 200240, People's Republic of China*

[4]*Center of Theoretical Nuclear Physics, National Laboratory of Heavy Ion Accelerator, Lanzhou 730000, People's Republic of China*

[5]*CCAST, World Laboratory, P. O. Box 8730, Beijing 100080, People's Republic of China*

(Received 26 June 2007; published 5 November 2007)

Systematic calculations on low-lying states are carried out for eighty odd-*A* nuclei with proton number ranging from 50 to 58 and neutron number from 74 to 90 by using the nucleon pair approximation. We use a separable phenomenological Hamiltonian that includes the monopole pairing, quadrupole pairing plus quadrupole-quadrupole interactions, with strength parameters exactly as those of the neighboring even-even nuclei. Our calculated energy spectra, electrical quadrupole moments, and magnetic *g* factors agree well with experimental data. Electromagnetic properties for low-lying states of these nuclei are discussed in detail.

DOI: 10.1103/PhysRevC.76.054305 PACS number(s): 21.10.Re, 21.60.Cs, 21.60.Ev, 23.20.Js

I. INTRODUCTION

An important question of nuclear structure theory is to describe low-lying states by using the shell model. Because the shell-model space for medium and heavy nuclei is usually too huge to handle, one needs truncation schemes to calculate low-lying collective states. The *sd* interacting boson model (IBM) [1] is a great success along this line. It stimulated many studies using collective *S* and *D* pairs, for example, the fermion dynamical symmetry model (FDSM) [2] which was established based on the famous Ginocchio model [3], the broken pair approximations (BPA) [4], the favored pair approximations (FPA) [5], and the nucleon pair approximation (NPA) [6,7], etc. Because the NPA can use arbitrary structures for its collective *S* and *D* pairs, it is flexible enough to include the BPA, the FPA, and the FDSM as its special cases. So far the NPA (and the Ginocchio model, the FDSM, the FPA, and the BPA) calculations concentrated largely on the structure of even-even nuclei, as the structure of odd-*A* nuclei is more complicated.

Among studies of odd-*A* nuclei based on nucleon pair truncation, the interacting boson fermion model (IBFM) [8] has been widely used, e.g., IBFM-1 calculations on odd-*A* Ba, Xe isotopes in Refs. [9–12], IBFM-2 calculations on odd-*A* Xe, Cs isotopes in Refs. [13,14], and on odd-*A* Ba, La isotopes in Ref. [15]. The FDSM was applied to describe low-lying states of odd-*A* nuclei with mass number *A* around 130 in Ref. [16], where positive-parity levels were reasonably reproduced and discussed. The NPA was applied to odd-*A* nuclei in Ref. [17] by Yoshinaga *et al*., who well reproduced energy spectra and magnetic moments of some odd-*A* Ba, Xe, Ce isotopes with $A \sim 130$.

In this article, we perform systematic NPA calculations for odd-*A* nuclei with $A \sim 130 - 150$. In Ref. [18], we calculated low-lying states for even-even nuclei with proton number ranging from 50 to 58, neutron number 74 to 90. This region is experimentally interesting, because Xe and Ba isotopes exhibit the O(6) behavior of the IBM when neutron number around 80–74, and $B(E2)$ values for ^{136}Te is exceptionally small. In Ref. [18], energy levels, $B(E2)$ values, and *g* factors are reasonably consistent with experimental data. It is therefore the purpose of this article to study the structure of their odd-*A* neighbors.

This article is organized as follows. In Sec. II we give a brief introduction of our framework that includes our basis, Hamiltonian, and electromagnetic transition operators. In Sec. III we discuss the pair structure coefficients and Hamiltonian parameters taken in this article. In Sec. IV our calculated results, including calculated low-energy spectra, electrical quadrupole moments Q, magnetic *g* factors, and some electromagnetic transitions, are presented and compared with experimental data. In Sec. V we summarize the results and conclusion of this article.

II. FRAMEWORK OF OUR CALCULATIONS

As in Refs. [6,7], our collective pair of spin *r* and projection μ is defined by

$$A^{r\dagger}_{\mu}|0\rangle = \sum_{ab} y(abr)(C^{\dagger}_{a} \times C^{\dagger}_{b})^{r}_{\mu}|0\rangle. \tag{1}$$

For an even-even nuclei, our model space is obtained by successively coupling collective pairs such defined. For an odd system with $2N+1$ nucleons, our basis is obtained by coupling N collective pairs $r_1, \ldots, r_N$ successively to an unpaired nucleon in j orbit, denoted by $A^{r_0\dagger}|0\rangle \equiv C^{\dagger}_{j}|0\rangle (r_0 = j)$, to obtain the total angular momentum J_N, with J_i (half-integer) as the angular momentum for the first $2i+1$ nucleons,

$$A^{J_N\dagger}_{M_N}(r_0 r_1 r_2 \cdots r_N, J_1 J_2 \cdots J_N) \equiv A^{J_N\dagger}_{M_N} = \{\cdots[(A^{r_0\dagger} \times A^{r_1\dagger})^{J_1} \times A^{r_2\dagger}]^{J_2} \times \cdots \times A^{r_N\dagger}\}^{J_N}_{M_N}. \tag{2}$$

*Present institution: Department of Physics and Astronomy and National Superconducting Cyclotron Laboratory, Michigan State University, East Lansing, Michigan 48824.

†Corresponding author: ymzhao@sjtu.edu.cn

If $A^{r_0\dagger} = 1$, it reduces to the basis for N pairs in an even system. We note that the above coupling procedure simplifies our calculations [7].

The Hamiltonian here is the same as that in our earlier calculations [18,19]. For the sake of completeness and convenience, we present its definition as follows.

$$H = H_0 + H_P + \kappa Q_\pi \cdot Q_\nu. \tag{3}$$

H_0 is the spherical single-particle energy term, and H_P is our residual interaction between like valence particles. Here

$$H_0 = \sum_{\alpha\sigma} \epsilon_{\alpha\sigma} C^\dagger_{\alpha\sigma} C_{\alpha\sigma},$$

$\sigma = \pi$ or ν, corresponding to the proton or neutron degree of freedom, respectively.

$$\begin{aligned} H_P &= V_0 + V_2 + V_Q, \\ V_0 &= G_\pi \mathcal{P}^\dagger_\pi \mathcal{P}_\pi + G_\nu \mathcal{P}^\dagger_\nu \mathcal{P}_\nu, \\ V_2 &= \sum_\sigma G^2_\sigma \mathcal{P}^{(2)\dagger}_\sigma \cdot \mathcal{P}^{(2)}_\sigma, \\ V_Q &= \sum_\sigma \kappa_\sigma Q_\sigma \cdot Q_\sigma, \end{aligned} \tag{4}$$

with

$$\begin{aligned} \mathcal{P}^\dagger_\sigma &= \sum_{a_\sigma} \frac{\sqrt{2a_\sigma + 1}}{2} \left(C^\dagger_{a_\sigma} \times C^\dagger_{a_\sigma}\right)^0_0, \\ \mathcal{P}^{(2)\dagger}_\sigma &= \sum_{a_\sigma b_\sigma} q(a_\sigma b_\sigma) \left(C^\dagger_{a_\sigma} \times C^\dagger_{b_\sigma}\right)^2, \\ Q_\sigma &= \sum_{a_\sigma b_\sigma} q(a_\sigma b_\sigma) \left(C^\dagger_{a_\sigma} \times \tilde{C}_{b_\sigma}\right)^2, \\ q(a_\sigma b_\sigma) &= \frac{(-)^{a_\sigma + 1/2}}{\sqrt{20\pi}} \hat{a}_\sigma \hat{b}_\sigma C^{20}_{a_\sigma 1/2, b_\sigma -1/2} \langle n_\sigma l_\sigma | r^2 | n_\sigma l'_\sigma \rangle. \end{aligned} \tag{5}$$

$\hat{j} = (2j+1)^{\frac{1}{2}}$, $C^{20}_{a1/2,b-1/2}$ is the Clebsch-Gordan coefficient. The matrix elements of r^2 are given in Ref. [20].

The $E2$ transition operator is

$$T(E2) = e_\pi Q_\pi + e_\nu Q_\nu, \tag{6}$$

where e_ν and e_π are effective charges of valence neutrons and valence protons, respectively.

The electrical quadrupole moment operator $\mathcal{Q}$ is

$$\mathcal{Q} = \sqrt{\frac{16\pi}{5}} T(E2). \tag{7}$$

The magnetic moment operator μ is

$$\mu = g_{l\pi} L_\pi + g_{l\nu} L_\nu + g_{s\pi} S_\pi + g_{s\nu} S_\nu, \tag{8}$$

where g_l and g_s are effective orbital and spin gyromagnetic ratios. The g factor for certain collective state is defined by μ/I, where I is the total spin of the collective state. The $M1$ transition operator is

$$T(M1) = \sqrt{\frac{3}{4\pi}} \mu, \tag{9}$$

The electrical $E2$ transition rate $B(E2)$, magnetic $M1$ transition rate $B(M1)$ are given by

$$\begin{aligned} B(E2) &= \frac{2I_f + 1}{2I_i + 1} \langle T(E2) \rangle^2, \\ B(M1) &= \frac{2I_f + 1}{2I_i + 1} \langle T(M1) \rangle^2, \end{aligned} \tag{10}$$

where I_f and I_i denote the angular momentum of the final state and initial state, respectively.

III. PARAMETERS OF THE HAMILTONIAN

As in Refs. [18,19], we use BCS pairs as our S pair. The D pair is obtained by using the commutator $D^\dagger = \frac{1}{2}[Q, S^\dagger]$, as suggested and studied in Ref. [21]. Here operator Q is defined in Eq. (5). We omit the script π or ν because we determine S and D pairs separately for protons and neutrons in the same way and this omission does not cause confusion.

Our single-particle energies ϵ_j of valence neutrons in the 50–82 shell are taken from experimental data of Ref. [22]. Our single-particle energies of valence neutrons in the 82–126 shell and valence protons are obtained from an extension of available experimental data from Refs. [23,24]. The values of ϵ_j were listed in Table I of Ref. [18] and are not repeated in this article.

In Ref. [18], we introduced a new procedure to find parameters of the Hamiltonian defined in Eq. (3). We fix our G_π, G_ν, and κ for all nuclei in the same shell and assume that G^2_π/κ_π and G^2_ν/κ_ν are constants when we adjusted parameters of the Hamiltonian. For example, for nuclei with valence neutrons in the 50–82 shell, we fix $G_\pi = -0.180$ MeV, $G_\nu = -0.131$ MeV, $\kappa = 0.06$ MeV/$r_0{}^4$. We define $G^2_\pi = -0.025\alpha_\pi$ MeV/$r_0{}^4$, $\kappa_\pi = -0.045\alpha_\pi$ MeV/$r_0{}^4$, $G^2_\nu = -0.013\alpha_\nu$ MeV/$r_0{}^4$, $\kappa_\nu = -0.015\alpha_\nu$ MeV/$r_0{}^4$. For nuclei with a single closed shell, we adjust α_π or α_ν to fit the experimental $E_{2^+_1}$. For cases with both valence protons and valence neutrons outside the core, α_π and α_ν are determined by experimental data of $E_{2^+_1}$, and parametrization of three single-closed nuclei, ^{134}Sn, ^{130}Te, and ^{134}Te through a phenomenological requirement. The same procedure was applied to cases with valence neutrons in the 82–126 shell in Ref. [18], where details can be found in Sec. III.

In this article we extend our calculations to odd-A nuclei of the same region by using the same Hamiltonian parameters as their even-even neighbors, namely we assume the same Hamiltonian parameters for an odd-A nucleus as those for its even-even "core". For convenience we list these parameters in Tables I and II.

IV. CALCULATED RESULTS

A. Energy spectra

Our calculated energy spectra and experimental values are presented in Figs. 1–4. Figure 1 refers to cases with an even value of proton number Z, an odd value of neutron number N, and both valence protons and valence neutrons in the 50–82 shell; Fig. 2 refers to cases with an odd Z but an even N and

TABLE I. Parameters for nuclei with both valence protons and valence neutrons in the 50–82 shell. They are the same as those in Ref. [18]. $G_\pi = -0.180$ MeV, $G_\nu = -0.131$ MeV, $\kappa = 0.06$ MeV/$r_0{}^4$ for all these nuclei. We define $G_\pi^2 = -0.025\alpha_\pi$ MeV/$r_0{}^4$, $\kappa_\pi = -0.045\alpha_\pi$ MeV/$r_0{}^4$, $G_\nu^2 = -0.013\alpha_\nu$ MeV/$r_0{}^4$, $\kappa_\nu = -0.015\alpha_\nu$ MeV/$r_0{}^4\alpha_\pi$ and α_ν are listed below for each nucleus. [a]

Nucl.	^{132}Sn,^{131}Sn,^{133}Sb	^{130}Sn,^{129}Sn,^{131}Sb	^{128}Sn,^{127}Sn,^{129}Sb	^{126}Sn,^{125}Sn,^{127}Sb	^{124}Sn ,^{125}Sb
α_ν	1.000	1.000	1.100	1.200	1.230
α_π	1.000	1.000	1.000	1.000	1.000
Nucl.	^{134}Te,^{133}Te,^{135}I	^{132}Te,^{131}Te,^{133}I	^{130}Te,^{129}Te,^{131}I	^{128}Te,^{127}Te,^{129}I	^{126}Te ,^{127}I
α_ν	1.000	1.170	1.353	1.512	1.673
α_π	1.000	1.130	1.190	1.250	1.330
Nucl.	^{136}Xe,^{135}Xe,^{137}Cs	^{134}Xe,^{133}Xe,^{135}Cs	^{132}Xe,^{131}Xe,^{133}Cs	^{130}Xe,^{129}Xe,^{131}Cs	^{128}Xe ,^{129}Cs
α_ν	1.000	1.320	1.540	1.764	1.980
α_π	0.920	1.113	1.187	1.279	1.371
Nucl.	^{138}Ba,^{137}Ba,^{139}La	^{136}Ba,^{135}Ba,^{137}La	^{134}Ba,^{133}Ba,^{135}La	^{132}Ba,^{131}Ba,^{133}La	^{130}Ba ,^{131}La
α_ν	1.000	1.370	1.595	1.812	2.103
α_π	0.850	1.071	1.148	1.224	1.352
Nucl.	^{140}Ce,^{139}Ce	^{138}Ce,^{137}Ce	^{136}Ce,^{135}Ce	^{134}Ce,^{133}Ce	^{132}Ce
α_ν	1.000	1.430	1.639	1.836	2.054
α_π	0.850	1.088	1.148	1.216	1.301

[a] α_π, α_ν for ^{134}Ba,^{134}Ce, and ^{132}Ce in Ref. [18] were misprinted. Their correct values are given in this table.

both valence protons and valence neutrons in the 50–82 shell; Fig. 3 refers to cases with an even Z and an odd N and valence protons in the 50–82 shell, valence neutrons in the 82–126 shell; Fig. 4 refers to cases with odd Z and even N, valence protons in the 50–82 shell and valence neutrons in the 82–126 shell. In these figures, experimental data are plotted on the left and calculated results on the right.

In Fig. 1, one sees that our calculations reproduce experimental energy levels well, both for positive-parity levels and negative-parity levels, except a few states such as the $7/2_2^+$ state in ^{127}Sn and ^{125}Sn. Our calculations also well reproduce the tendency of relative positions between the lowest two states, $3/2_1^+$ and $1/2_1^+$, for these nuclei. When the number of valence neutrons (holelike) is small, the ground-state spin is $3/2_1^+$, because the unpaired neutron hole stays on the lowest neutron single hole state $3/2^+$. As the valence proton number and the valence neutron number increase, the second lowest state $1/2_1^+$ goes close to the ground state $3/2_1^+$; as valence nucleon numbers continue to increase, it goes below the $3/2_1^+$ state and becomes the ground state. The two states $3/2_1^+$ and $1/2_1^+$ change their sequence around ^{129}Xe, ^{133}Ba, and ^{135}Ce, according to experimental data. Our calculations are nicely consistent with those data. For negative-parity levels, a similar phenomenon occurs between $11/2_1^-$ and $9/2_1^-$ states, i.e., the $9/2_1^-$ state goes down below the $11/2_1^-$ state around ^{131}Ba and ^{133}Ce as the valence nucleon number increases. Although our calculation does not lower $9/2_1^-$ down as large as experimental data, the tendency is reproduced. The calculation by

TABLE II. Parameters for nuclei with valence protons in the 50–82 shell and valence neutrons in the 82–126 shell. They are the same as those in Ref. [18]. $G_\pi = -0.150$ MeV, $G_\nu = -0.131$ MeV, $\kappa = -0.06$ MeV/$r_0{}^4$ for all these nuclei. We define $G_\pi^2 = -0.0177\alpha_\pi$ MeV/$r_0{}^4$, $\kappa_\pi = -0.032\alpha_\pi$ MeV/$r_0{}^4$, $G_\nu^2 = -0.0135\alpha_\nu$ MeV/$r_0{}^4$, $\kappa_\nu = -0.015\alpha_\nu$ MeV/$r_0{}^4$. α_π and α_ν are listed below for each nucleus.

Nucl.	^{132}Sn,^{133}Sn,^{133}Sb	^{134}Sn,^{135}Sn,^{135}Sb	^{136}Sn,^{137}Sn,^{137}Sb	^{138}Sn,^{139}Sn,^{139}Sb	^{140}Sn ,^{141}Sb
α_ν	1.000	1.000	1.050	1.105	1.140
α_π	1.000	1.000	1.000	1.000	1.000
Nucl.	^{134}Te,^{135}Te,^{135}I	^{136}Te,^{137}Te,^{137}I	^{138}Te,^{139}Te,^{139}I	^{140}Te,^{141}Te,^{141}I	^{142}Te ,^{143}I
α_ν	1.000	1.100	1.197	1.249	1.288
α_π	1.000	1.300	1.520	1.540	1.540
Nucl.	^{136}Xe,^{137}Xe,^{137}Cs	^{138}Xe,^{139}Xe,^{139}Cs	^{140}Xe,^{141}Xe,^{141}Cs	^{142}Xe,^{143}Xe,^{143}Cs	^{144}Xe ,^{145}Cs
α_ν	1.000	1.100	1.208	1.315	1.368
α_π	0.840	1.134	1.327	1.504	1.588
Nucl.	^{138}Ba,^{139}Ba,^{139}La	^{140}Ba,^{141}Ba,^{141}La	^{142}Ba,^{143}Ba,^{143}La	^{144}Ba,^{145}Ba,^{145}La	^{146}Ba ,^{147}La
α_ν	1.000	1.080	1.197	1.392	1.414
α_π	0.750	0.990	1.208	1.665	1.650
Nucl.	^{140}Ce,^{141}Ce	^{142}Ce,^{143}Ce	^{144}Ce,^{145}Ce	^{146}Ce,^{147}Ce	^{148}Ce
α_ν	1.000	1.040	1.103	1.216	1.425
α_π	1.020	1.122	1.153	1.295	2.448

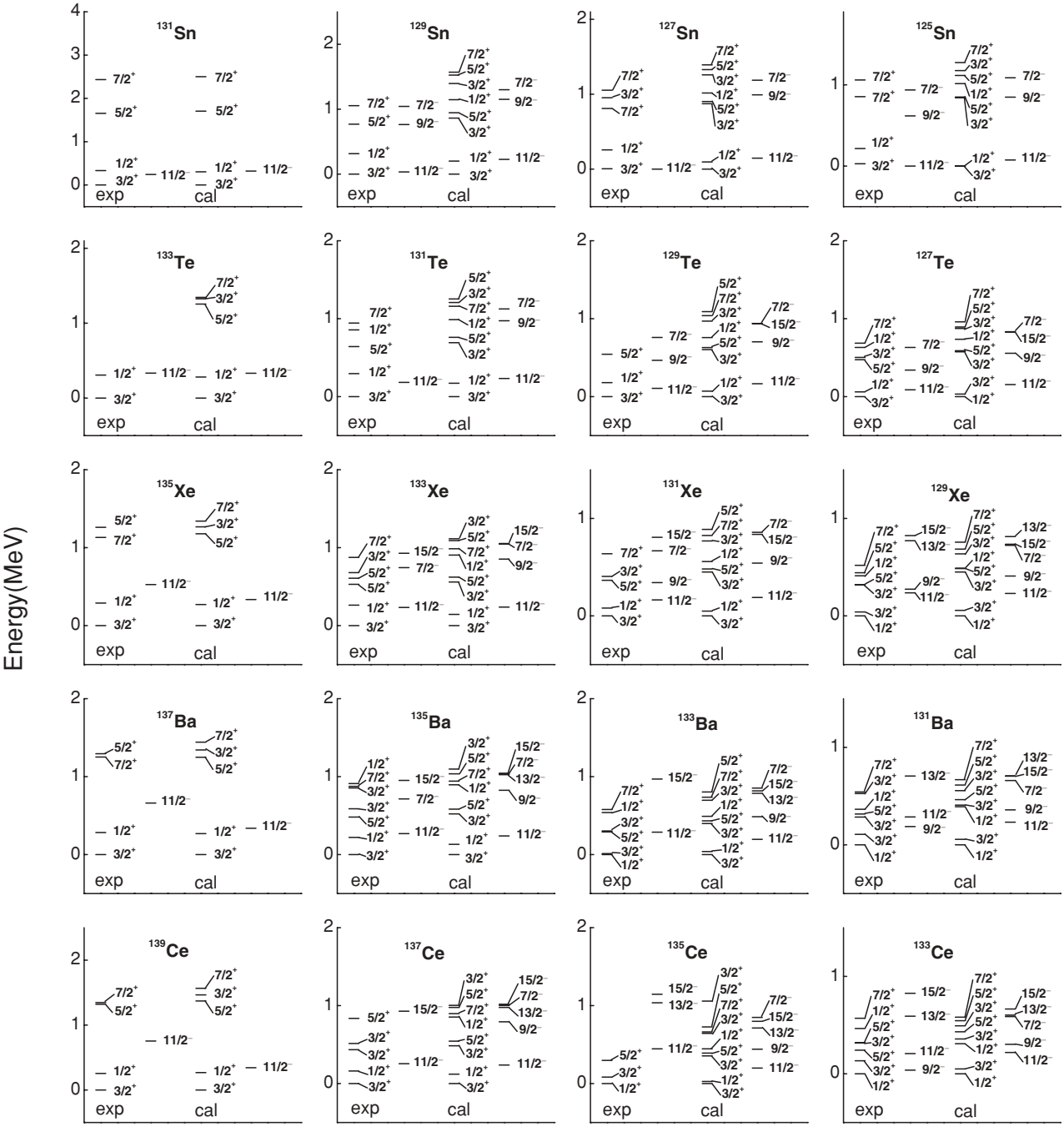

FIG. 1. The energy spectra of proton-even neutron-odd nuclei with both valence protons and valence neutrons in the 50–82 shell. The left side of each figure is plotted based on the experimental data taken from Ref. [24], whereas the right side is plotted based on our calculated results.

Yoshinaga *et al.* in Ref. [17] can reproduce this $11/2^-_1, 9/2^-_1$ reordering, but their calculated negative-parity levels seems much lower than experimental results. This reordering phenomenon is worthy of further studies in future.

In Fig. 2, our calculations also well reproduce experimental data in general. In this case there exists a similar reordering of the ground-state spin from $7/2^+_1$ to $5/2^+_1$, as valence nucleon numbers increase. Our calculations reproduce such a phenomenon. However, our calculated negative-parity levels are systematically higher than their experimental values. This may be because our proton single-particle energy for $11/2^-_1$ level (2.76 MeV) is larger than it should be. When there are many valence protons and neutrons, our calculated $11/2^-_1$ states are lowered below 2 MeV, but not low enough. Furthermore, we should note that the two lowest $5/2^+$ states of our calculation are close to each other and should change their order. This can be seen from their electromagnetic properties in Table IV, which will be explained in the next subsection.

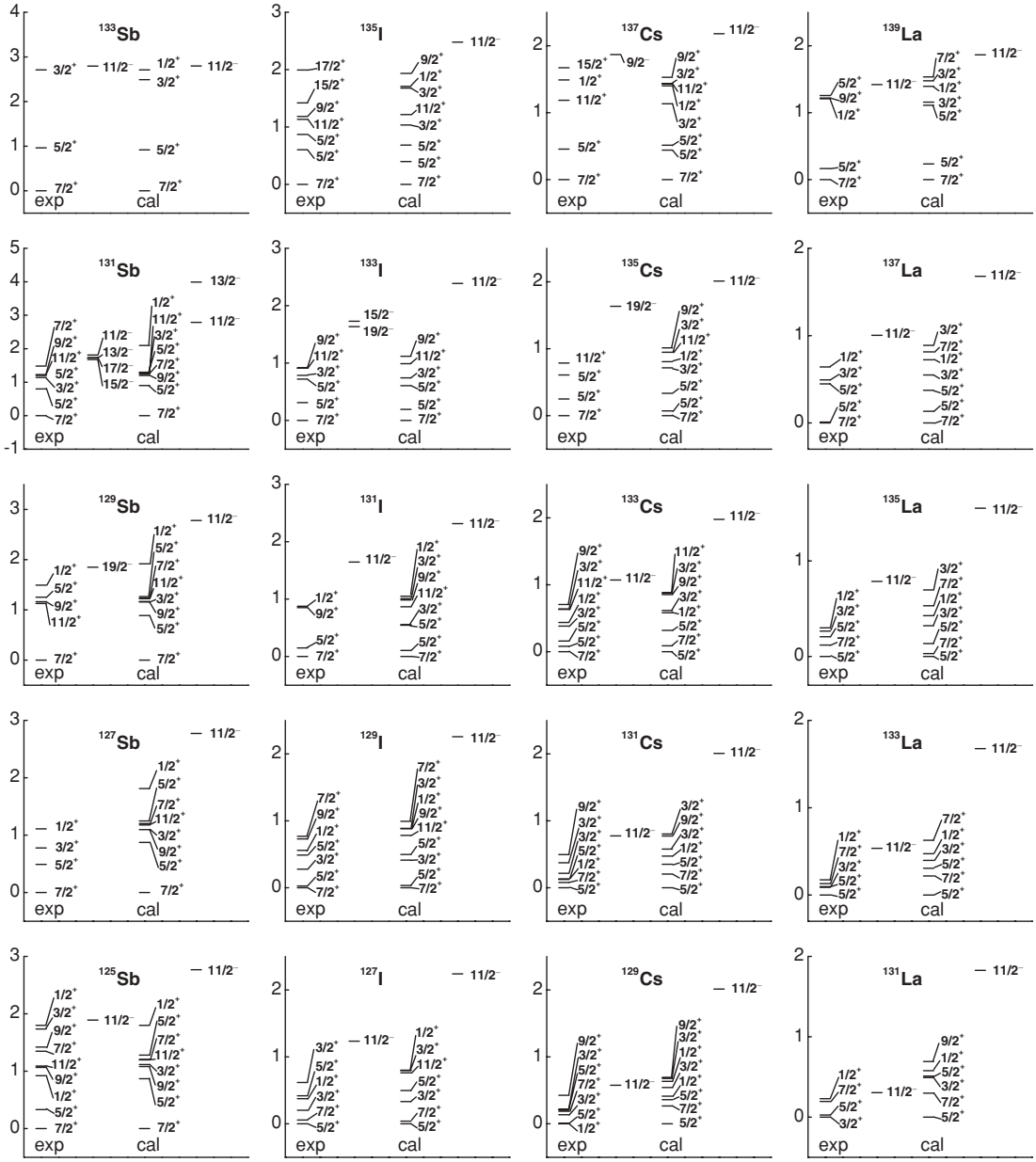

FIG. 2. The same to Fig. 1 except for nuclei with odd-valence protons in the 50–82 shell and even-valence neutrons in the 50–82 shell.

In Fig. 3 our calculations agree well with experimental results. Most negative-parity levels are well reproduced in our calculations. The nearly degenerate "triplet" ground state, $3/2_1^-$, $5/2_1^-$, and $7/2_1^-$, of ^{139}Xe, ^{141}Ba, and ^{143}Ce appears in our calculated levels. But the calculated positive-parity state $13/2_1^+$ is slightly higher than experimental data, and the calculated decreasing tendency of the $13/2_1^+$ state is not as large as that of the experiment.

In Fig. 4, our calculated results are not satisfactorily consistent with experimental data. For example, $3/2_1^+$ is not the ground state for ^{143}Cs and ^{145}Cs nuclei while it is the ground state according to experimental data. Also the calculated electric quadruple moments $\mathcal{Q}$ of the $7/2_1^+$ state for ^{139}Cs and ^{141}Cs are not consistent with experimental data.

B. Electromagnetic properties

In this work we do not adjust our effective charges in Eq. (6) or effective g factors in Eq. (8). We use the same values for effective charges and g factors as those for their even-even neighbors taken in our previous article [18]: $e_\pi = 1.9389e$ and $e_\nu = -1.0795e$ for nuclei with valence protons in the 50–82 shell and valence neutrons in the 50–82 shell; $e_\pi = 1.9389e$ and $e_\nu = 1.0795e$ for those with valence protons in the 50–82 shell and valence neutrons in the 82–126 shell. These effective charges are obtained in Ref. [18] via the χ^2-squared fitting procedure considering *only even-even nuclei* in this region. We use $g_{l\pi} = 1\ \mu_N$, $g_{l\nu} = 0$, $g_{s\pi} = 5.586 \times 0.7\ \mu_N$, $g_{s\nu} = -3.826 \times 0.7\ \mu_N$, i.e., free nucleon g factors with the spin

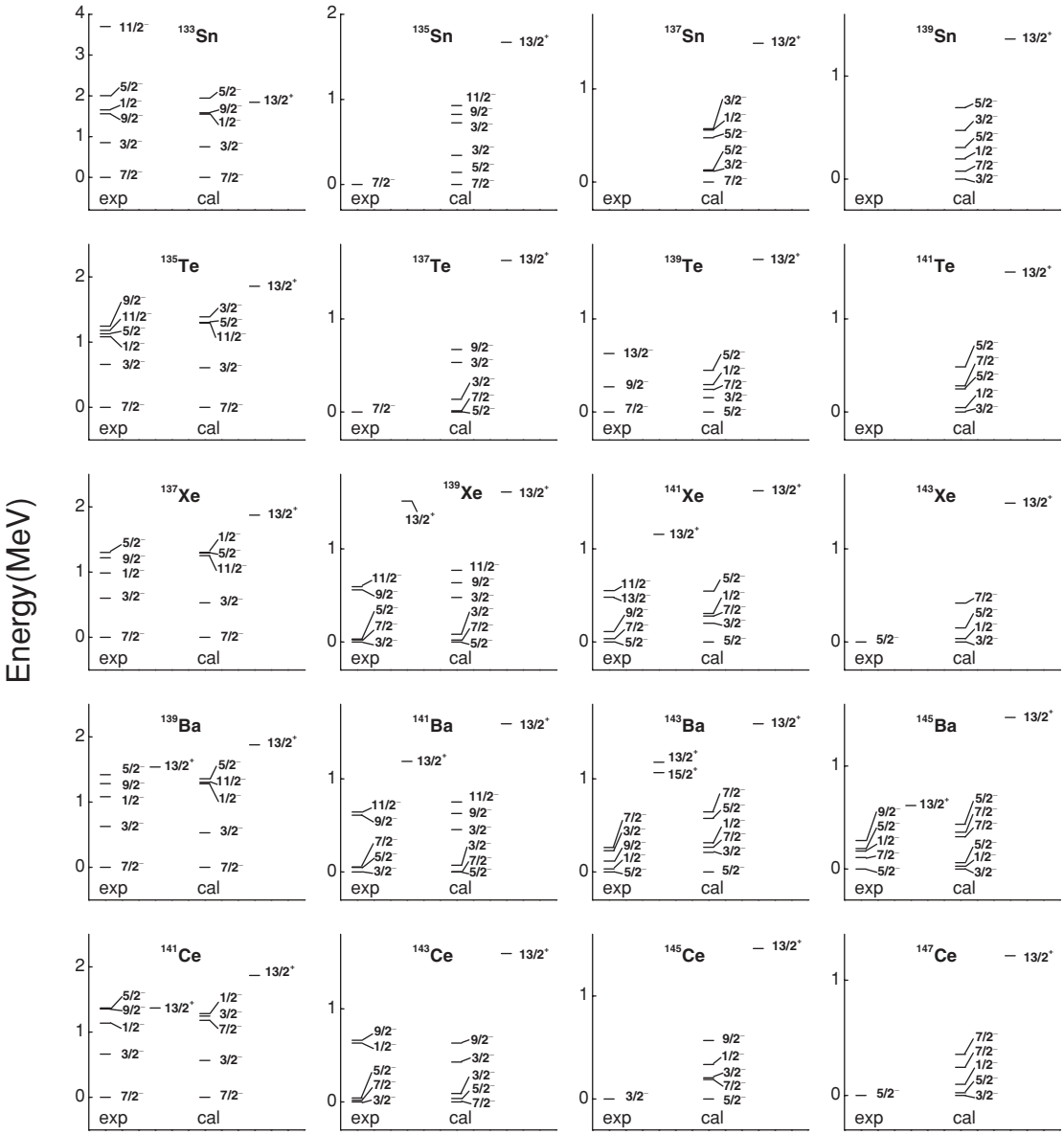

FIG. 3. The same to Fig. 1 except for nuclei with even-valence protons in the 50–82 shell and odd-valence neutrons in the 82–126 shell.

part multiplied by a factor of 0.7 (conventional quenching factor).

We present our calculated results of electrical quadrupole moment $\mathcal{Q}$, magnetic moment μ in Tables III–VI (as in Ref. [25], we write signs of μ and $\mathcal{Q}$ explicitly if they were known based on previous experiments; otherwise we list only their magnitudes). Some $E2$ and $M1$ transition rates for ^{129}Xe, ^{131}Xe are given in Table VII and compared with other calculations (the IBFM-1 [9] and the FDSM [2]). Our calculated results are compared with available experimental data in Tables III–VII. One sees that our calculated $\mathcal{Q}$, μ, $E2$, and $M1$ transition rates are well consistent with available experimental data except a few cases, which will be discussed as below.

As in Sec. IV A, our calculated results of μ and $\mathcal{Q}$ are good for cases with an even Z and an odd N, and valence neutrons in the 50–82 shell, i.e., the same nuclei in Fig. 1. In Table III, one sees that our calculated quadrupole moments $\mathcal{Q}$ and g factors are close to available experimental data. Our calculations also reproduce the decreasing tendency of $\mathcal{Q}$ and g factor of the $3/2^+_1$ state in Xe isotopes, as the valence neutrons (holes) increase. In particular, experimental values of $\mathcal{Q}$ moment for the $3/2^+_1$ state change in a large range from $+0.214(7)$ to $-0.41(4)$, and our calculation presents both the correct signs and reasonable magnitudes for all these nuclei.

In Table IV we present results of $\mathcal{Q}$ and g factor of nuclei with an odd Z but an even N, both valence protons and neutrons in the 50–82 shell. One sees that our calculations also reproduce tendencies of $\mathcal{Q}$ and g factor for the $7/2^+_1$ state, except g factor of $7/2^+_1$ state for ^{139}La and ^{137}La nuclei. We point out that we should treat the lowest two $5/2^+$ states of experimental data in reverse order for ^{133}Cs, ^{131}Cs, according to calculated values in Table IV. Namely our calculated lowest two $5/2^+$ states of ^{133}Cs, ^{131}Cs are not in the correct order. If

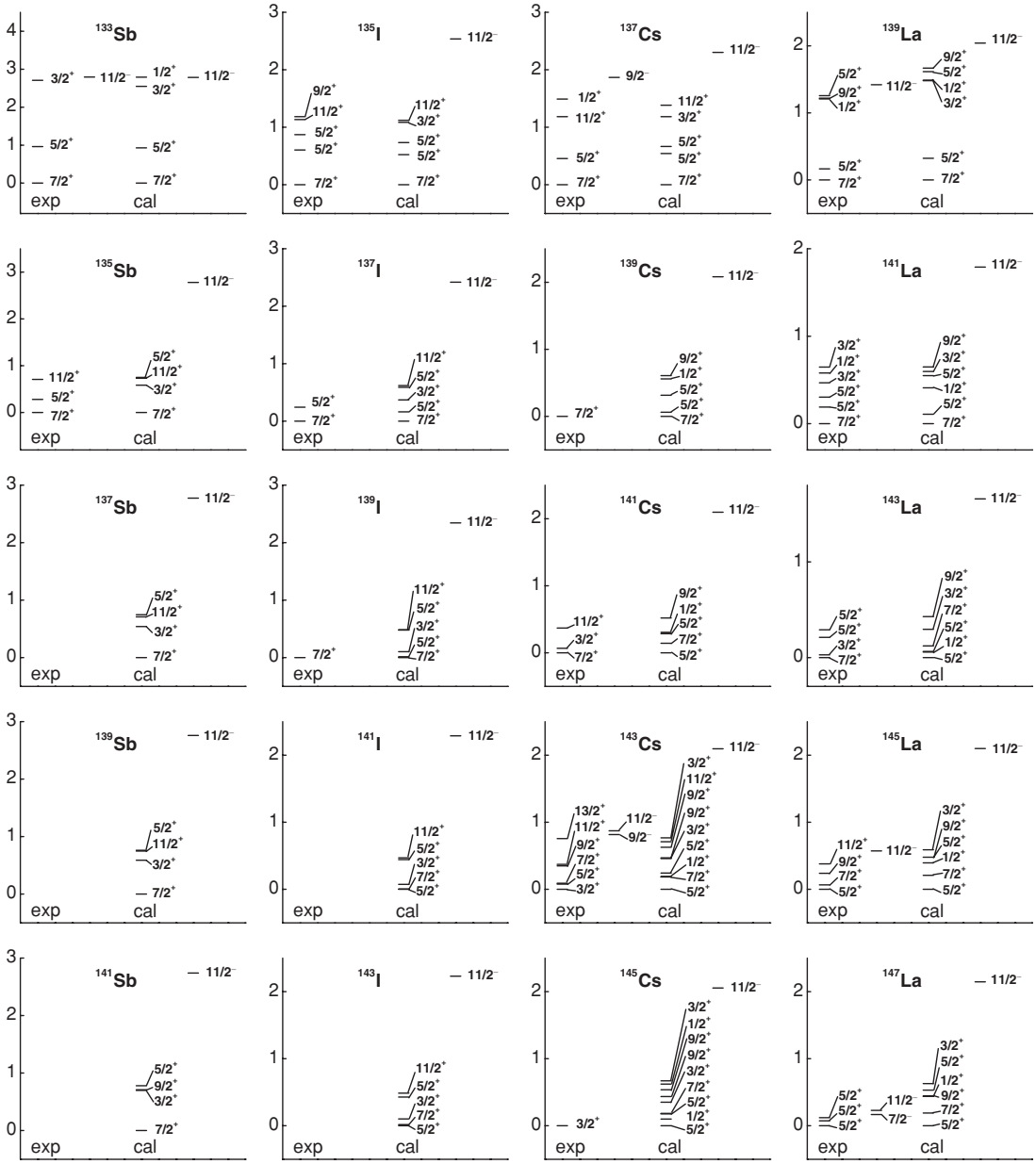

FIG. 4. The same to Fig. 1 except for nuclei with odd-valence protons in the 50–82 shell and even-valence neutrons in the 82–126 shell.

one examines $\mathcal{Q}$ and g factors of La isotopes in Table IV, it is easy to notice that there is a reordering of the lowest two $5/2^+$ states that appears around ^{137}La and ^{135}La, according to our calculations.

Calculated results of $\mathcal{Q}$ and g factor for nuclei with valence neutrons in the 82–126 shell are given in Tables V and VI. In general our calculation reproduces the experimental data, although calculated g factors for $3/2^-_1$ states in Table V are systematically larger in magnitude compared with the available experimental data. As for Table VI, although the calculated g factors agree with the experiment, our calculated $\mathcal{Q}$ moments have large discrepancies with the experiment, some of them even have an opposite sign. Especially, the experimental $3/2^+_1$ state is the ground state in ^{143}Cs, ^{145}Cs, and has a very low excitation energy in ^{141}Cs and ^{143}La. Our calculated $3/2^+_1$ states of these nuclei are not low enough, implying certain physics not included in our calculation. Consequently, the calculated $\mathcal{Q}$ and g factor of these $3/2^+$ states are not good. Because our calculated g factors of the $3/2^+_1$ state at ^{143}Cs and ^{145}Cs are too small compared with the experimental data, we list $3/2^+_2$ instead of $3/2^+_1$. They are separate by approximately 0.3 MeV.

In Table VII we investigate $E2$ and $M1$ transition rates. One can see that our calculations present $B(E2)$ well but not so well for $B(M1)$ [especially for $B(M1)$ of ^{129}Xe], similar to the IBFM1 calculation in Ref. [9]. If we adjust Hamiltonian parameters of this nucleus, we are able to improve the agreement between calculated results of $B(M1)$ and their experimental data. Here we would like to mention, however, an improvement of our calculation compared with the work

TABLE III. g factors and electrical quadrupole moments $\mathcal{Q}$ of the proton-even neutron-odd nuclei in the proton 50–82, neutron 50–82 shell. g factor is calculated with effective g factors $g_{l\pi} = 1\ \mu_N$, $g_{lv} = 0$, $g_{s\pi} = 5.586 \times 0.7\ \mu_N$, $g_{sv} = -3.826 \times 0.7\ \mu_N$, and listed in unit of μ_N. $\mathcal{Q}$ moment is calculated with effective charges $e_\pi = 1.9389e$, $e_v = -1.0795e$, and listed in unit of eb. If we cannot determine the sign of an experimental value, we list only its magnitude. Experimental data are taken from [a]Ref. [26], [b]Ref. [27], [c]Ref. [28], [d]Ref. [29], [e]Ref. [30], [f]Ref. [31], [g]Ref. [25], [h]Ref. [32], [i]Ref. [33], [j]Ref. [34], [k]Ref. [35], [l]Ref. [36], [m]Ref. [37], [n]Ref. [38], [o]Ref. [39], [p]Ref. [25], [q]Ref. [25], [r]Ref. [40].

	g factor		$\mathcal{Q}$ moment			g factor		$\mathcal{Q}$ moment	
	Cal.	Exp.	Cal.	Exp.		Cal.	Exp.	Cal.	Exp.
^{131}Sn $1/2_1^+$	−2.678	–	–	–	^{131}Xe $1/2_1^+$	−1.885	–	–	–
$3/2_1^+$	+0.536	–	+0.121	–	$3/2_1^+$	+0.437	+0.461[g]	−0.203	−0.120(12)[h]
$5/2_1^+$	−0.536	–	+0.172	–	$5/2_1^+$	+0.196	–	−0.145	–
$9/2_1^-$	–	–	–	–	$9/2_1^-$	−0.271	–	+0.569	–
$11/2_1^-$	−0.243	–	+0.274	–	$11/2_1^-$	−0.235	−0.181[g]	+0.447	+0.73(3)[g]
^{129}Sn $1/2_1^+$	−2.500	–	–	–	^{129}Xe $1/2_1^+$	−1.177	−1.556[i]	–	–
$3/2_1^+$	+0.507	–	+0.025	–	$3/2_1^+$	+0.362	+0.387[j]	−0.380	−0.41(4)[k]
$5/2_1^+$	+0.024	–	−0.039	–	$5/2_1^+$	+0.161	–	−0.065	–
$9/2_1^-$	−0.256	–	+0.195	–	$9/2_1^-$	−0.267	–	+0.395	–
$11/2_1^-$	−0.243	–	+0.232	–	$11/2_1^-$	−0.230	−0.162[g]	+0.229	+0.64(2)[g]
^{127}Sn $1/2_1^+$	−2.298	–	–	–	^{137}Ba $1/2_1^+$	−2.573	–	–	–
$3/2_1^+$	+0.483	–	−0.043	–	$3/2_1^+$	+0.560	+0.625[l]	+0.229	0.246(2)[m]
$5/2_1^+$	+0.029	–	−0.003	–	$5/2_1^+$	+0.712	–	−0.230	–
$9/2_1^-$	−0.256	–	+0.153	–	$9/2_1^-$	−0.354	–	+0.678	–
$11/2_1^-$	−0.243	–	+0.174	–	$11/2_1^-$	−0.238	−0.180[n]	+0.598	+0.78(9)[n]
^{125}Sn $1/2_1^+$	−2.102	–	–	–	^{135}Ba $1/2_1^+$	−2.230	–	–	–
$3/2_1^+$	+0.460	–	−0.096	–	$3/2_1^+$	+0.527	+0.559[l]	+0.042	+0.160(3)[o]
$5/2_1^+$	+0.027	–	+0.051	–	$5/2_1^+$	+0.289	–	−0.220	–
$9/2_1^-$	−0.255	–	+0.048	–	$9/2_1^-$	−0.272	–	+0.642	–
$11/2_1^-$	−0.243	−0.245[a]	+0.105	+0.1(2)[a]	$11/2_1^-$	−0.234	−0.182[n]	+0.677	+0.98(8)[n]
^{133}Te $1/2_1^+$	−2.588	–	–	–	^{133}Ba $1/2_1^+$	−1.843	−1.554[n]	–	–
$3/2_1^+$	+0.552	–	+0.183	–	$3/2_1^+$	+0.441	+0.340[p]	−0.247	–
$5/2_1^+$	+0.706	–	−0.094	–	$5/2_1^+$	+0.222	–	−0.218	–
$9/2_1^-$	−0.357	–	+0.321	–	$9/2_1^-$	−0.271	–	+0.745	–
$11/2_1^-$	−0.240	–	+0.439	–	$11/2_1^-$	−0.231	−0.165[n]	+0.541	+0.89(7)[n]
^{131}Te $1/2_1^+$	−2.401	–	–	–	^{131}Ba $1/2_1^+$	−1.082	−1.416[q]	–	–
$3/2_1^+$	+0.515	0.464[b]	+0.034	–	$3/2_1^+$	+0.376	–	−0.447	–
$5/2_1^+$	+0.185	–	−0.091	–	$5/2_1^+$	+0.177	–	−0.172	–
$9/2_1^-$	−0.271	–	+0.340	–	$9/2_1^-$	−0.267	−0.193[n]	+0.565	+1.46(13)[n]
$11/2_1^-$	−0.240	−0.189[c]	+0.407	–	$11/2_1^-$	−0.223	–	+0.260	–
^{129}Te $1/2_1^+$	−2.062	–	–	–	^{139}Ce $1/2_1^+$	−2.579	–	–	–
$3/2_1^+$	+0.458	0.468[b]	−0.118	0.055(13)[d]	$3/2_1^+$	+0.561	0.707[r]	+0.233	–
$5/2_1^+$	+0.154	–	−0.050	–	$5/2_1^+$	+0.706	–	−0.215	–
$9/2_1^-$	−0.269	–	+0.323	–	$9/2_1^-$	−0.358	–	+0.765	–
$11/2_1^-$	−0.240	−0.198[b]	+0.313	–	$11/2_1^-$	−0.238	–	+0.593	–
^{127}Te $1/2_1^+$	−1.616	–	–	–	^{137}Ce $1/2_1^+$	−2.170	–	–	–
$3/2_1^+$	+0.401	0.423[b]	−0.235	–	$3/2_1^+$	+0.531	0.640[r]	+0.040	–
$5/2_1^+$	+0.134	–	+0.027	–	$5/2_1^+$	+0.321	–	−0.256	–
$9/2_1^-$	−0.267	−0.218[e]	+0.174	–	$9/2_1^-$	−0.270	–	+0.732	–
$11/2_1^-$	−0.239	−0.189[f]	+0.183	–	$11/2_1^-$	−0.232	0.184[r]	+0.763	–
^{135}Xe $1/2_1^+$	−2.563	–	–	–	^{135}Ce $1/2_1^+$	−1.788	–	–	–
$3/2_1^+$	+0.559	+0.602[g]	+0.218	+0.214(7)[g]	$3/2_1^+$	+0.453	–	−0.296	–
$5/2_1^+$	+0.709	–	−0.190	–	$5/2_1^+$	+0.260	–	−0.299	–
$9/2_1^-$	−0.354	–	+0.538	–	$9/2_1^-$	−0.270	–	+0.936	–
$11/2_1^-$	−0.238	−0.187[g]	+0.561	+0.62(2)[g]	$11/2_1^-$	−0.225	–	+0.648	–
^{133}Xe $1/2_1^+$	−2.280	–	–	–	^{133}Ce $1/2_1^+$	−1.025	–	–	–
$3/2_1^+$	+0.521	+0.542[g]	+0.037	+0.142(5)[g]	$3/2_1^+$	+0.409	–	−0.521	–
$5/2_1^+$	+0.261	–	−0.173	–	$5/2_1^+$	+0.202	–	−0.352	–
$9/2_1^-$	−0.273	–	+0.529	–	$9/2_1^-$	−0.269	–	+0.769	–
$11/2_1^-$	−0.236	−0.197[g]	+0.578	+0.77(3)[g]	$11/2_1^-$	−0.212	–	+0.307	–

TABLE IV. g factors and electrical quadrupole moments $\mathcal{Q}$ of the proton-odd neutron-even nuclei in the proton 50–82, neutron 50–82 shell. Note that our calculated $5/2_1^+, 5/2_2^+$ levels are very likely in the wrong energy order, based on their electromagnetic properties. g factor is calculated with effective g factors $g_{l\pi} = 1\ \mu_N$, $g_{lv} = 0$, $g_{s\pi} = 5.586 \times 0.7\ \mu_N$, $g_{sv} = -3.826 \times 0.7\ \mu_N$, and listed in unit of μ_N. $\mathcal{Q}$ moment is calculated with effective charges $e_\pi = 1.9389e$, $e_v = -1.0795e$, and listed in unit of eb. If we cannot determine the sign of an experimental value, we only list its magnitude. Experimental data are taken from [a]Ref. [41], [b]Ref. [42], [c]Ref. [43], [d]Ref. [25], [e]Ref. [44], [f]Ref. [45], [g]Ref. [46], [h]Ref. [47], [i]Ref. [48], [j]Ref. [49], [k]Ref. [25], [l]Ref. [50], [m]Ref. [51], [n]Ref. [52], [o]Ref. [53], [p]Ref. [54], [q]Ref. [55], [r]Ref. [56], [s]Ref. [57], [t]Ref. [58], [u]Ref. [25], [v]Ref. [59], [w]Ref. [60], [x]Ref. [61], [y]Ref. [62], [z]Ref. [63], [A]Ref. [25].

	g factor		$\mathcal{Q}$ moment			g factor		$\mathcal{Q}$ moment	
	Cal.	Exp.	Cal.	Exp.		Cal.	Exp.	Cal.	Exp.
^{133}Sb $3/2_1^+$	+0.418	–	−0.218	–	^{137}Cs $3/2_1^+$	+0.610	–	−0.226	–
$5/2_1^+$	+1.582	–	−0.311	–	$5/2_1^+$	+1.301	–	−0.189	–
$5/2_2^+$	–	–	–	–	$5/2_2^+$	+0.957	–	+0.290	–
$7/2_1^+$	+0.677	0.857[a]	−0.363	–	$7/2_1^+$	+0.677	+0.811[n]	+0.105	+0.03(4)[n]
$11/2_1^-$	+1.265	–	−0.495	–	$11/2_1^-$	+1.263	–	−0.728	–
^{131}Sb $3/2_1^+$	+1.259	–	−0.137	–	^{135}Cs $3/2_1^+$	+0.774	–	−0.178	–
$5/2_1^+$	+1.538	–	−0.377	–	$5/2_1^+$	+0.699	–	+0.533	–
$5/2_2^+$	+0.748	–	−0.189	–	$5/2_2^+$	+1.496	–	−0.514	–
$7/2_1^+$	+0.671	0.826[a]	−0.446	–	$7/2_1^+$	+0.663	+0.780[n]	+0.139	+0.03(2)[n]
$11/2_1^-$	+1.259	–	−0.613	–	$11/2_1^-$	+1.251	–	−1.016	–
^{129}Sb $3/2_1^+$	+1.236	–	−0.181	–	^{133}Cs $3/2_1^+$	+0.770	–	−0.160	–
$5/2_1^+$	+1.499	–	−0.427	–	$5/2_1^+$	+0.681	+1.380[o]	+0.633	−0.33(2)[p]
$5/2_2^+$	+0.767	–	−0.188	–	$5/2_2^+$	+1.428	+0.800[q]	−0.636	–
$7/2_1^+$	+0.665	0.797[b]	−0.512	–	$7/2_1^+$	+0.638	+0.737[r]	+0.142	−0.00371(14)[s]
$11/2_1^-$	+1.255	–	−0.705	–	$11/2_1^-$	+1.239	–	−1.206	–
^{127}Sb $3/2_1^+$	+1.218	–	−0.207	–	^{131}Cs $3/2_1^+$	+0.674	–	−0.167	–
$5/2_1^+$	+1.464	–	−0.467	–	$5/2_1^+$	+0.664	+1.416[n]	+0.722	−0.575(6)[t]
$5/2_2^+$	+0.784	–	−0.211	–	$5/2_2^+$	+1.332	+0.744[u]	−0.721	–
$7/2_1^+$	+0.661	0.771[b]	−0.566	–	$7/2_1^+$	+0.598	–	+0.138	–
$11/2_1^-$	+1.251	–	−0.781	–	$11/2_1^-$	+1.227	–	−1.357	–
^{125}Sb $3/2_1^+$	+1.200	–	−0.218	–	^{129}Cs $3/2_1^+$	+0.573	–	−0.169	–
$5/2_1^+$	+1.457	–	−0.494	–	$5/2_1^+$	+0.650	–	+0.782	–
$5/2_2^+$	+0.782	–	−0.242	–	$5/2_2^+$	+1.232	–	−0.771	–
$7/2_1^+$	+0.658	+0.751[c]	−0.598	–	$7/2_1^+$	+0.557	–	+0.145	–
$11/2_1^-$	+1.248	–	−0.828	–	$11/2_1^-$	+1.214	+1.191[v]	−1.483	–
^{135}I $3/2_1^+$	+0.476	–	+0.015	–	^{139}La $3/2_1^+$	+1.104	–	+0.106	–
$5/2_1^+$	+0.681	–	−0.133	–	$5/2_1^+$	+1.572	–	−0.351	–
$5/2_2^+$	+1.570	–	−0.371	–	$5/2_2^+$	+0.719	–	+0.628	–
$7/2_1^+$	+0.676	–	−0.138	–	$7/2_1^+$	+0.677	+1.112[w]	+0.353	+0.20(1)[x]
$11/2_1^-$	+1.263	–	−0.656	–	$11/2_1^-$	+1.263	–	−0.733	–
^{133}I $3/2_1^+$	+0.525	–	+0.070	–	^{137}La $3/2_1^+$	+1.254	–	+0.215	–
$5/2_1^+$	+0.670	–	−0.168	–	$5/2_1^+$	+1.455	–	−0.480	+0.26(8)[y]
$5/2_2^+$	+1.541	–	−0.495	–	$5/2_2^+$	+0.770	–	+0.781	–
$7/2_1^+$	+0.665	+0.816[d]	−0.174	−0.24(1) [e]	$7/2_1^+$	+0.667	+1.078[z]	+0.492	+0.26(8)[z]
$11/2_1^-$	+1.254	–	−0.865	–	$11/2_1^-$	+1.250	–	−1.080	–
^{131}I $3/2_1^+$	+0.576	–	+0.144	–	^{135}La $3/2_1^+$	+1.270	–	+0.287	–
$5/2_1^+$	+0.661	+1.120[f]	−0.193	–	$5/2_1^+$	+0.830	–	+0.551	–
$5/2_2^+$	+1.506	–	−0.590	–	$5/2_2^+$	+1.306	–	−0.210	–
$7/2_1^+$	+0.650	+0.783[g]	−0.214	−0.35(2)[g]	$7/2_1^+$	+0.648	–	+0.499	–
$11/2_1^-$	+1.245	–	−1.022	–	$11/2_1^-$	+1.238	–	−1.294	–
^{129}I $3/2_1^+$	+0.588	–	+0.190	–	^{133}La $3/2_1^+$	+1.266	–	+0.352	–
$5/2_1^+$	+0.652	+1.122[h]	−0.219	−0.42(2)[i]	$5/2_1^+$	+0.677	–	+1.020	–
$5/2_2^+$	+1.472	–	−0.664	–	$5/2_2^+$	+1.361	–	−0.654	–
$7/2_1^+$	+0.633	+0.749[j]	−0.246	−0.482(10)[e]	$7/2_1^+$	+0.613	–	+0.327	–
$11/2_1^-$	+1.236	–	−1.151	–	$11/2_1^-$	+1.227	1.364[A]	−1.447	–
^{127}I $3/2_1^+$	+0.565	+0.647[k]	+0.186	–	^{131}La $3/2_1^+$	+1.271	–	+0.444	–
$5/2_1^+$	+0.643	+1.125[j]	−0.251	−0.789[l]	$5/2_1^+$	+0.650	–	+1.145	–
$5/2_2^+$	+1.438	–	−0.723	–	$5/2_2^+$	+1.255	–	−0.767	–
$7/2_1^+$	+0.612	+0.726[m]	−0.258	−0.62(2)[e]	$7/2_1^+$	+0.569	–	+0.240	–
$11/2_1^-$	+1.226	–	−1.263	–	$11/2_1^-$	+1.213	–	−1.582	–

TABLE V. g factors and electrical quadrupole moments $\mathcal{Q}$ of the proton-even neutron-odd nuclei in the proton 50–82, neutron 82–126 shell. g factor is calculated with effective g factors $g_{l\pi} = 1\ \mu_N$, $g_{lv} = 0$, $g_{s\pi} = 5.586 \times 0.7\ \mu_N$, $g_{sv} = -3.826 \times 0.7\ \mu_N$, and listed in unit of μ_N. $\mathcal{Q}$ moment is calculated with effective charges $e_\pi = 1.9389e$, $e_v = 1.0795e$, and listed in unit of eb. If we can not determine the sign of an experimental value, we list only its magnitude. Experimental data are taken from [a]Ref. [64], [b]Ref. [39], [c]Ref. [65], [d]Ref. [25].

	g factor		$\mathcal{Q}$ moment			g factor		$\mathcal{Q}$ moment	
	Cal.	Exp.	Cal.	Exp.		Cal.	Exp.	Cal.	Exp.
^{133}Sn $3/2_1^-$	−0.893	–	−0.143	–	^{141}Xe $3/2_1^-$	−0.492	–	−0.412	–
$5/2_1^-$	+0.383	–	−0.205	–	$5/2_1^-$	−0.296	–	+0.885	–
$7/2_1^-$	−0.383	–	−0.239	–	$7/2_1^-$	−0.227	–	+0.166	–
$9/2_1^+$	–	–	–	–	$9/2_1^+$	−0.345	–	−0.819	–
$13/2_1^+$	−0.206	–	−0.331	–	$13/2_1^+$	−0.198	–	−1.032	–
^{135}Sn $3/2_1^-$	−0.706	–	−0.095	–	^{143}Xe $3/2_1^-$	−0.298	–	−0.491	–
$5/2_1^-$	−0.403	–	−0.020	–	$5/2_1^-$	−0.250	−0.184[a]	+1.021	+0.93(3)[a]
$7/2_1^-$	−0.374	–	−0.056	–	$7/2_1^-$	−0.252	–	+0.865	–
$9/2_1^+$	−0.268	–	−0.398	–	$9/2_1^+$	−0.324	–	−0.896	–
$13/2_1^+$	−0.206	–	−0.415	–	$13/2_1^+$	−0.196	–	−1.155	–
^{137}Sn $3/2_1^-$	−0.622	–	−0.184	–	^{139}Ba $3/2_1^-$	−0.991	–	−0.293	–
$5/2_1^-$	−0.321	–	+0.450	–	$5/2_1^-$	−0.266	–	−0.023	–
$7/2_1^-$	−0.360	–	+0.128	–	$7/2_1^-$	−0.364	−0.278[b]	−0.441	−0.573(13)[b]
$9/2_1^+$	−0.267	–	−0.449	–	$9/2_1^+$	−0.595	–	−0.646	–
$13/2_1^+$	−0.206	–	−0.481	–	$13/2_1^+$	−0.203	–	−0.570	–
^{139}Sn $3/2_1^-$	−0.613	–	−0.230	–	^{141}Ba $3/2_1^-$	−0.638	−0.225[b]	+0.270	+0.454(10)[b]
$5/2_1^-$	−0.286	–	+0.172	–	$5/2_1^-$	−0.365	–	−0.040	–
$7/2_1^-$	−0.332	–	+0.308	–	$7/2_1^-$	−0.322	–	−0.258	–
$9/2_1^+$	−0.266	–	−0.432	–	$9/2_1^+$	−0.395	–	−0.743	–
$13/2_1^+$	−0.205	–	−0.535	–	$13/2_1^+$	−0.199	–	−0.873	–
^{135}Te $3/2_1^-$	−0.978	–	−0.213	–	^{143}Ba $3/2_1^-$	−0.466	–	−0.476	–
$5/2_1^-$	−0.417	–	−0.004	–	$5/2_1^-$	−0.293	–	+0.967	–
$7/2_1^-$	−0.371	–	−0.366	–	$7/2_1^-$	−0.186	–	+0.159	–
$9/2_1^+$	−0.594	–	−0.377	–	$9/2_1^+$	−0.375	–	−0.905	–
$13/2_1^+$	−0.204	–	−0.496	–	$13/2_1^+$	−0.195	–	−1.129	–
^{137}Te $3/2_1^-$	−0.655	–	+0.047	–	^{145}Ba $3/2_1^-$	−0.194	–	−0.590	–
$5/2_1^-$	−0.389	–	−0.030	–	$5/2_1^-$	−0.226	−0.114[b]	+1.183	+1.22(2)[b]
$7/2_1^-$	−0.349	–	−0.129	–	$7/2_1^-$	−0.025	–	+0.118	–
$9/2_1^+$	−0.321	–	−0.571	–	$9/2_1^+$	−0.341	–	−1.023	–
$13/2_1^+$	−0.202	–	−0.687	–	$13/2_1^+$	−0.191	–	−1.297	–
^{139}Te $3/2_1^-$	−0.525	–	−0.278	–	^{141}Ce $3/2_1^-$	−0.984	–	−0.301	–
$5/2_1^-$	−0.296	–	+0.717	–	$5/2_1^-$	−0.159	–	−0.136	–
$7/2_1^-$	−0.304	–	+0.182	–	$7/2_1^-$	−0.366	0.311[c]	−0.413	–
$9/2_1^+$	−0.308	–	−0.678	–	$9/2_1^+$	−0.625	–	−0.755	–
$13/2_1^+$	−0.201	–	−0.845	–	$13/2_1^+$	−0.204	–	−0.544	–
^{141}Te $3/2_1^-$	−0.403	–	−0.350	–	^{143}Ce $3/2_1^-$	−0.622	0.287[d]	+0.378	–
$5/2_1^-$	−0.260	–	+0.646	–	$5/2_1^-$	−0.342	–	−0.053	–
$7/2_1^-$	−0.279	–	+0.623	–	$7/2_1^-$	−0.315	–	−0.279	–
$9/2_1^+$	−0.301	–	−0.717	–	$9/2_1^+$	−0.442	–	−0.848	–
$13/2_1^+$	−0.200	–	−0.940	–	$13/2_1^+$	−0.198	–	−0.910	–
^{137}Xe $3/2_1^-$	−1.002	–	−0.271	–	^{145}Ce $3/2_1^-$	−0.454	–	−0.560	–
$5/2_1^-$	−0.342	–	+0.020	–	$5/2_1^-$	−0.299	–	+1.072	–
$7/2_1^-$	−0.364	−0.277[a]	−0.434	−0.48(2)[a]	$7/2_1^-$	−0.185	–	+0.128	–
$9/2_1^+$	−0.589	–	−0.549	–	$9/2_1^+$	−0.430	–	−1.040	–
$13/2_1^+$	−0.203	–	−0.567	–	$13/2_1^+$	−0.192	–	−1.254	–
^{139}Xe $3/2_1^-$	−0.641	−0.203[a]	+0.210	+0.40(2)[a]	^{147}Ce$3/2_1^-$	−0.312	–	−0.707	–
$5/2_1^-$	−0.374	–	−0.035	–	$5/2_1^-$	−0.260	–	+1.336	–
$7/2_1^-$	−0.327	–	−0.224	–	$7/2_1^-$	−0.087	–	+0.265	–
$9/2_1^+$	−0.374	–	−0.684	–	$9/2_1^+$	−0.400	–	−1.147	–
$13/2_1^+$	−0.200	–	−0.832	–	$13/2_1^+$	−0.188	–	−1.436	–

TABLE VI. g factors and electrical quadrupole moments $\mathcal{Q}$ of the proton-odd neutron-even nuclei in the proton 50–82, neutron 82–126 shell. Note that we list $3/2_2^+$ instead of $3/2_1^+$ at ^{143}Cs and ^{145}Cs, because our calculated g factors of the $3/2_1^+$ state for these two nuclei are too small compared with the experimental data. g factor is calculated with effective g factors $g_{l\pi} = 1\ \mu_N$, $g_{lv} = 0$, $g_{s\pi} = 5.586 \times 0.7\ \mu_N$, $g_{sv} = -3.826 \times 0.7\ \mu_N$, and listed in unit of μ_N. $\mathcal{Q}$ moment is calculated with effective charges $e_\pi = 1.9389e$, $e_v = 1.0795e$, and listed in unit of eb. If we cannot determine the sign of an experimental value, we only list its magnitude. Experimental data are taken from [a]Ref. [41], [b]Ref. [52], [c]Ref. [60], [d]Ref. [61].

	g factor		$\mathcal{Q}$ moment			g factor		$\mathcal{Q}$ moment	
	Cal.	Exp.	Cal.	Exp.		Cal.	Exp.	Cal.	Exp.
^{133}Sb $3/2_1^+$	+0.418	–	−0.218	–	^{137}Cs $3/2_1^+$	+0.619	–	−0.239	–
$5/2_1^+$	+1.582	–	−0.311	–	$5/2_1^+$	+1.566	–	−0.373	–
$7/2_1^+$	+0.677	0.857[a]	−0.363	–	$7/2_1^+$	+0.676	+0.811[b]	+0.107	+0.03(4)[b]
$11/2_1^-$	+1.265	–	−0.495	–	$11/2_1^-$	+1.264	–	−0.656	–
$15/2_1^-$	–	–	–	–	$15/2_1^-$	+1.154	–	−0.940	–
^{135}Sb $3/2_1^+$	+1.224	–	−0.204	–	^{139}Cs $3/2_1^+$	+0.916	–	−0.027	–
$5/2_1^+$	+0.846	–	−0.076	–	$5/2_1^+$	+0.664	–	+0.688	–
$7/2_1^+$	+0.662	–	−0.504	–	$7/2_1^+$	+0.651	+0.771[b]	+0.129	−0.06(3)[b]
$11/2_1^-$	+1.255	–	−0.671	–	$11/2_1^-$	+1.249	–	−1.019	–
$15/2_1^-$	+0.918	–	−0.719	–	$15/2_1^-$	+1.011	–	−1.151	–
^{137}Sb $3/2_1^+$	+1.195	–	−0.268	–	^{141}Cs $3/2_1^+$	+0.583	–	−0.228	–
$5/2_1^+$	+0.915	–	−0.215	–	$5/2_1^+$	+0.638	–	+0.880	–
$7/2_1^+$	+0.652	–	−0.608	–	$7/2_1^+$	+0.576	+0.691[b]	+0.130	−0.45(7)[b]
$11/2_1^-$	+1.247	–	−0.806	–	$11/2_1^-$	+1.233	–	−1.256	–
$15/2_1^-$	+0.911	–	−0.868	–	$15/2_1^-$	+0.983	–	−1.385	–
^{139}Sb $3/2_1^+$	+1.172	–	−0.306	–	^{143}Cs $3/2_2^+$	+0.615	+0.580[b]	+0.444	+0.47(3)[b]
$5/2_1^+$	+0.996	–	−0.368	–	$5/2_1^+$	+0.616	–	+1.004	–
$7/2_1^+$	+0.645	–	−0.689	–	$7/2_1^+$	+0.497	–	+0.164	–
$11/2_1^-$	+1.239	–	−0.924	–	$11/2_1^-$	+1.216	–	−1.436	–
$15/2_1^-$	+0.905	–	−0.919	–	$15/2_1^-$	+0.962	–	−1.559	–
^{141}Sb $3/2_1^+$	+1.154	–	−0.320	–	^{145}Cs $3/2_2^+$	+0.635	+0.523[b]	−0.422	+0.62(6)[b]
$5/2_1^+$	+1.067	–	−0.496	–	$5/2_1^+$	+0.606	–	+1.092	–
$7/2_1^+$	+0.641	–	−0.753	–	$7/2_1^+$	+0.462	–	+0.189	–
$11/2_1^-$	+1.233	–	−1.028	–	$11/2_1^-$	+1.204	–	−1.586	–
$15/2_1^-$	+0.899	–	−0.843	–	$15/2_1^-$	+0.950	–	−1.702	–
^{135}I $3/2_1^+$	+0.517	–	+0.075	–	^{139}La $3/2_1^+$	+1.225	–	+0.170	–
$5/2_1^+$	+0.669	–	−0.151	–	$5/2_1^+$	+1.579	–	−0.350	–
$7/2_1^+$	+0.676	–	−0.133	–	$7/2_1^+$	+0.677	+0.795[c]	+0.357	+0.20(1)[d]
$11/2_1^-$	+1.264	–	−0.623	–	$11/2_1^-$	+1.264	–	−0.640	–
$15/2_1^-$	+1.157	–	−0.677	–	$15/2_1^-$	+1.159	–	−1.068	–
^{137}I $3/2_1^+$	+0.818	–	+0.245	–	^{141}La $3/2_1^+$	+1.295	–	+0.197	–
$5/2_1^+$	+0.662	–	−0.097	–	$5/2_1^+$	+1.502	–	−0.617	–
$7/2_1^+$	+0.650	–	−0.242	–	$7/2_1^+$	+0.659	–	+0.615	–
$11/2_1^-$	+1.250	–	−0.910	–	$11/2_1^-$	+1.250	–	−1.036	–
$15/2_1^-$	+0.969	–	−0.970	–	$15/2_1^-$	+1.025	–	−1.227	–
^{139}I $3/2_1^+$	+0.733	–	+0.395	–	^{143}La $3/2_1^+$	+0.999	–	+0.016	–
$5/2_1^+$	+0.625	–	−0.155	–	$5/2_1^+$	+1.200	–	−0.394	–
$7/2_1^+$	+0.601	–	−0.337	–	$7/2_1^+$	+0.620	–	+0.526	–
$11/2_1^-$	+1.234	–	−1.117	–	$11/2_1^-$	+1.233	–	−1.323	–
$15/2_1^-$	+0.950	–	−1.186	–	$15/2_1^-$	+1.008	–	−1.491	–
^{141}I $3/2_1^+$	+0.708	–	+0.463	–	^{145}La $3/2_1^+$	+0.221	–	−0.457	–
$5/2_1^+$	+0.606	–	−0.235	–	$5/2_1^+$	+0.607	–	+1.345	–
$7/2_1^+$	+0.579	–	−0.371	–	$7/2_1^+$	+0.485	–	+0.256	–
$11/2_1^-$	+1.222	–	−1.276	–	$11/2_1^-$	+1.209	–	−1.535	–
$15/2_1^-$	+0.938	–	−1.320	–	$15/2_1^-$	+0.981	–	−1.695	–
^{143}I $3/2_1^+$	+0.688	–	+0.507	–	^{147}La $3/2_1^+$	−0.019	–	−0.615	–
$5/2_1^+$	+0.604	–	−0.332	–	$5/2_1^+$	+0.594	–	+1.460	–
$7/2_1^+$	+0.569	–	−0.369	–	$7/2_1^+$	+0.457	–	+0.280	–
$11/2_1^-$	+1.211	–	−1.423	–	$11/2_1^-$	+1.199	–	−1.670	–
$15/2_1^-$	+0.931	–	−1.401	–	$15/2_1^-$	+0.965	–	−1.837	–

TABLE VII. $E2$ and $M1$ transition rates of ^{129}Xe and ^{131}Xe. $B(E2)$ is calculated with effective charges $e_\pi = 1.9389\,e$, $e_\nu = -1.0795\,e$, and listed in units of $10^{-3}\,e^2\mathrm{b}^2$. $B(M1)$ is calculated with effective g factors $g_{l\pi} = 1\ \mu_N$, $g_{l\nu} = 0$, $g_{s\pi} = 5.586 \times 0.7\ \mu_N$, $g_{s\nu} = -3.826 \times 0.7\ \mu_N$, and listed in unit of $10^{-3}\mu_N^2$. The IBFM calculated results are taken from Ref. [9] and the FDSM results are taken from Ref. [2]. Experimental data are taken from Refs. [66–68].

		$B(E2)$				$B(M1)$		
	$J_i \to J_f$	NPA	IBFM	FDSM	Exp.	NPA	IBFM	Exp.
^{129}Xe	$\frac{3}{2}^+_1 \to \frac{1}{2}^+_1$	7.865	11	36	–	33.67	0.1	49(2)
	$\frac{3}{2}^+_2 \to \frac{3}{2}^+_1$	17.41	27	18.6	< 0.5	40.32	0.1	8(1)
	$\frac{3}{2}^+_2 \to \frac{1}{2}^+_1$	100.1	101	84	120(10)	20.65	0.1	1.8(2)
	$\frac{5}{2}^+_1 \to \frac{3}{2}^+_1$	80.24	85	11	220(30)	5.050	29.9	17(3)
	$\frac{5}{2}^+_1 \to \frac{1}{2}^+_1$	31.24	52	70	77(7)	–	–	–
	$\frac{1}{2}^+_2 \to \frac{3}{2}^+_2$	29.67	24	28	–	28.26	4.6	12(4)
	$\frac{1}{2}^+_2 \to \frac{3}{2}^+_1$	123.8	80	140	44(11)	2.744	0.2	4.5(8)
	$\frac{1}{2}^+_2 \to \frac{1}{2}^+_1$	–	–	–	–	146.9	1.1	4.5(8)
	$\frac{5}{2}^+_2 \to \frac{1}{2}^+_1$	88.51	67	4	57(4)	–	–	–
	$\frac{3}{2}^+_3 \to \frac{1}{2}^+_1$	15.89	11	56	3.2(2)	18.77	0.1	–
	$\frac{3}{2}^+_4 \to \frac{1}{2}^+_1$	0.4542	1	13.3	3.0(2)	18.60	0.1	–
^{131}Xe	$\frac{1}{2}^+_1 \to \frac{3}{2}^+_1$	5.198	9	95.3	3.9(5)	23.29	–	–
	$\frac{5}{2}^+_1 \to \frac{1}{2}^+_1$	30.90	28	75	30(5)	–	–	–
	$\frac{5}{2}^+_1 \to \frac{3}{2}^+_1$	89.96	80	4	100(10)	9.8804	34.2	0.64(12)
	$\frac{3}{2}^+_2 \to \frac{3}{2}^+_1$	67.89	65	53	57(4)	23.48	0.1	<7
	$\frac{1}{2}^+_2 \to \frac{1}{2}^+_1$	–	–	–	–	44.030	–	>1
	$\frac{1}{2}^+_2 \to \frac{3}{2}^+_1$	95.85	70	124	48(4)	11.42	0.2	–
	$\frac{7}{2}^+_1 \to \frac{5}{2}^+_1$	7.935	3	28	5	0.06871	10.2	2(1)
	$\frac{7}{2}^+_1 \to \frac{3}{2}^+_1$	100.5	92	43	81(6)	–	–	–
	$\frac{3}{2}^+_3 \to \frac{3}{2}^+_1$	17.43	22	25	27(2)	6.435	0.3	–
	$\frac{5}{2}^+_2 \to \frac{3}{2}^+_2$	15.55	6	4	<31	75.78	35.2	58(6)
	$\frac{5}{2}^+_2 \to \frac{1}{2}^+_1$	76.89	71	71	68(9)	–	–	–
	$\frac{5}{2}^+_2 \to \frac{3}{2}^+_1$	15.25	19	14	13(1)	73.29	49.5	108(8)
	$\frac{7}{2}^+_2 \to \frac{3}{2}^+_1$	0.01346	0.2	124	5.0(5)	–	–	–

in Ref. [9]. A detailed analysis of the $B(M1)$ transition $\frac{3}{2}^+_1 \to \frac{1}{2}^+_1$ of ^{129}Xe has been made in Ref. [9], concerning the disagreement between the calculated $B(M1, \frac{3}{2}^+_1 \to \frac{1}{2}^+_1)$ by the IBFM1 and experimental data. Our calculation of this quantity is very close to the experimental result.

We also perform a χ^2-squared fitting to obtain effective g factors in Eq. (8) by taking into experimental data of magnetic g factors for both even-even and odd-A nuclei of this region. Our effective g factors are $g_{l\pi} = 1.013\ \mu_N$, $g_{l\nu} = 0.044\ \mu_N$. $g_{s\pi} = 5.586 \times 0.612\ \mu_N$, $g_{s\nu} = -3.826 \times 0.612\ \mu_N$. The standard derivation by using this set of g factors is $0.140\ \mu_N$, in comparison with the standard derivation ($0.156\ \mu_N$) by using $g_{l\pi} = 1\ \mu_N$, $g_{l\nu} = 0$ and $g_{s\pi} = 5.586 \times 0.7\ \mu_N$, $g_{s\nu} = -3.826 \times 0.7\ \mu_N$. These two sets of parameters are very close to each other.

V. DISCUSSION AND SUMMARY

In this article we extend our calculation of low-lying states for even-even nuclei with proton number Z ranging from 50 to 58 and neutron number N ranging from 74 to 90 to their odd-A neighbors. We use the same parameters, including the Hamiltonian interaction strengths, effective charges, and effective g factors, for odd-A nuclei as their even-even neighbors taken in Ref. [18], where we assumed that G_π^2/κ_π and G_ν^2/κ_ν are constants when we adjusted parameters of the Hamiltonian. We calculate energy spectra, electrical quadrupole moments $\mathcal{Q}$, magnetic g factors, etc., for 80 odd-A nuclei in this region. The calculated results are well consistent with experimental data, except for a few cases (e.g., the electrical quadrupole moment $\mathcal{Q}$ of $7/2^+_1$ in ^{141}Cs) that deserve further studies in future.

We also present many calculated results, such as energy levels, quadrupole moments, and g factors, of low-lying states for cases where few data are available and expect that our calculations will be useful in future experiments.

ACKNOWLEDGMENTS

The authors are very grateful to Professor A. Arima for many discussions and to Mr. Y. Lei and Mr. Z. Y. Xu for checking numerical results of this article by independent computer codes. We thank the National Natural Science Foundation of China for supporting this work under

grants 10575070 and 10675081. This work is also supported partly by the Research Foundation Doctoral Program of Higher Education of China under grant no. 20060248050, Scientific Research Foundation of Ministry of Education in China for Returned Scholars, and by Chinese Major State Basic Research Developing Program under Grant 2007CB815000.

[1] A. Arima and F. Iachello, Ann. Phys. **99**, 253 (1976); **111**, 201 (1978); **123**, 468 (1979); for a review, see F. Iachello and A. Arima, *The Interacting Boson Model* (Cambridge, UK, Cambridge University Press, 1987).
[2] C. L. Wu, D. H. Feng, X. G. Chen, J. Q. Chen, and M. Guidry, Phys. Rev. C **36**, 1157 (1987).
[3] J. N. Ginocchio, Ann. Phys. **126**, 234 (1980); A. Arima, J. N. Ginoccio, and N. Yoshida, Nucl. Phys. **A384**, 112 (1982).
[4] Y. K. Gambir, S. Haq, and J. K. Suri, Ann. Phys. (NY) **133**, 154 (1981).
[5] K. T. Hecht, J. B. McGrory, and J. P. Draayer, Nucl. Phys. **A197**, 369 (1972).
[6] J. Q. Chen, Nucl. Phys. **A626**, 686 (1997).
[7] Y. M. Zhao, N. Yoshinaga, S. Yamaji, J. Q. Chen, and A. Arima, Phys. Rev. C **62**, 014304 (2000).
[8] F. Iachello and P. Van Isacker, *The Interacting Boson-Fermion Model* (Cambridge, UK, Cambridge University Press, 1991).
[9] M. A. Cunningham, Nucl. Phys. **A385**, 204 (1982); **A385**, 221 (1982).
[10] H. C. Chiang, S. T. Hsieh, and D. S. Chuu, Phys. Rev. C **39**, 2390 (1989).
[11] S. T. Hsieh, H. C. Chiang, and M. M. King Yen, Phys. Rev. C **41**, 2898 (1990).
[12] D. Bucurescu, G. Cata-Danil, N. V. Zamfir, A. Gizon, and J. Gizon, Phys. Rev. C **43**, 2610 (1991).
[13] J. M. Arias, C. E. Alonso, and R. Bijker, Nucl. Phys. **A445**, 333 (1985).
[14] N. Yoshida, A. Gelberg, T. Otsuka, I. Wiedenhover, H. Sagawa, and P. von Brentano, Nucl. Phys. **A619**, 65 (1997).
[15] C. E. Alonso, J. M. Arias, and M. Lozano, J. Phys. G **13**, 1269 (1987).
[16] X. W. Pan, J. L. Ping, D. H. Feng, J. Q. Chen, C. L. Wu, and M. W. Guidry, Phys. Rev. C **53**, 715 (1996).
[17] N. Yoshinaga and K. Higashiyama, Phys. Rev. C **69**, 054309 (2004).
[18] L. Y. Jia, H. Zhang, and Y. M. Zhao, Phys. Rev. C **75**, 034307 (2007).
[19] Y. M. Zhao, S. Yamaji, N. Yoshinaga, and A. Arima, Phys. Rev. C **62**, 014315 (2000); Y. M. Zhao, N. Yoshinaga, S. Yamaji, and A. Arima, *ibid*. **C62**, 024322 (2000).
[20] S. Yoshida, Phys. Rev. **123**, 2122 (1961).
[21] K. Allart, E. Boeker, G. Bonsignori, M. Saroia, and Y. K. Gambhir, Phys. Rep. **169**, 209 (1988); I. Talmi, Nucl. Phys. **A172**, 1 (1972).
[22] B. Fogelberg and J. Blomqvist, Nucl. Phys. **A429**, 205 (1984).
[23] W. J. Baldridge, Phys. Rev. C **18**, 530 (1978).
[24] ENSDF Viewer, National Nuclear Data Center, http://ie.lbl.gov/ensdf/
[25] N. J. Stone, At. Data Nucl. Data Tables **90**, 75 (2005).
[26] M. Anselment, K. Bekk, A. Hanser, H. Hoeffgen, G. Meisel, S. Goring, H. Rebel, and G. Schatz, Phys. Rev. C **34**, 1052 (1986).
[27] R. Geerts, C. Nuytten, E. Schoeters, R. Silverans, and L. Vanneste, Phys. Rev. C **20**, 1171 (1979).
[28] G. Lhersonneau, J. De Raedt, H. Van de Voorde, H. Ooms, R. Haroutunian, E. Schoeters, R. E. Silverans, and L. Vanneste, Phys. Rev. C **12**, 609 (1975).
[29] I. Berkes, O. El Hajjaji, M. Fahad, B. Hlimi, G. Marest, H. Sayouty, G. Langouche, M. Van Der Heyden, and M. Tong, Hyperfine Interact. **35**, 1023 (1987).
[30] Maristela Olzon M. D. de Souza and R. N. Saxena, Phys. Rev. C **31**, 593 (1985).
[31] R. Geerts, C. Nuytten, E. Schoeters, R. Silverans, and L. Vanneste, Phys. Rev. C **21**, 439 (1980).
[32] W. L. Faust and M. N. McDermott, Phys. Rev. **123**, 198 (1961).
[33] D. Brinkmann, Helv. Phys. Acta **41**, 367 (1968).
[34] F. Janig and F. Brochard, J. Phys. (Paris) **35**, 301 (1974).
[35] Gilbert J. Perlow, Phys. Rev. **135**, B1102 (1964).
[36] O. Lutz and H. Oehler, Z. Phys. A **288**, 11 (1978).
[37] Roger E. Silverans, Gustaaf Borghs, Peter De Bisschop, and Marleen Van Hove, Phys. Rev. A **33**, 2117 (1986).
[38] A. C. Mueller, F. Buchinger, W. Klempt, E. W. Otten, R. Neugart, C. Ekstrom, and J. Heinemeier, Nucl. Phys. **A403**, 234 (1983).
[39] K. Wendt, S. A. Ahmad, C. Ekstrom, W. Klempt, R. Neugart, and E. W. Otten, Z. Phys. A **329**, 407 (1988).
[40] Suguru Muto, Susumu Ohya, Kazuhiko Heiguchi, and Naoshi Mutsuro, J. Phys. Soc. Jpn. **60**, 845 (1991).
[41] N. J. Stone, D. Doran, M. Lindroos, J. Rikovska, M. Veskovic, G. White, D. A. Williams, B. Fogelberg, L. Jacobsson, I. S. Towner, and K. Heyde, Phys. Rev. Lett. **78**, 820 (1997).
[42] M. Lindroos, M. Booth, D. Doran, Y. Koh, I. Oliveira, J. Rikovska, P. Richards, N. J. Stone, M. Veskovic, D. Zakoucky, and B. Fogelberg, Phys. Rev. C **53**, 124 (1996).
[43] P. T. Callaghan, M. Shott, and N. J. Stone, Nucl. Phys. **A221**, 1 (1974).
[44] Heinz Haas and Helena M. Petrilli, Phys. Rev. B **61**, 13588 (2000).
[45] P. N. Tandon and H. G. Devare, Nucl. Phys. **A102**, 203 (1967).
[46] Edgar Lipworth, Hugh L. Garvin, and Thomas M. Green, Phys. Rev. **119**, 2022 (1960).
[47] H. de Waard and G. Calis, Phys. Lett. **B106**, 457 (1979).
[48] M. Grodzicki, V. Manning, A. X. Trautwein, and J. M. Friedt, J. Phys. B **20**, 5595 (1987).
[49] Harold Walchli, Ralph Livingston, and Gordon Herbert, Phys. Rev. **82**, 97 (1951).
[50] Gladys H. Fuller, J. Phys. Chem. Ref. Data **5**, 835 (1976).
[51] N. S. Wolmarans and H. de Waard, Phys. Rev. C **6**, 228 (1972).
[52] C. Thibault, F. Touchard, S. Buttgenbach, R. Klapisch, M. De Saint Simon, H. T. Duong, P. Jacquinot, P. Juncar, S. Liberman, P. Pillet, J. Pinard, J. L. Vialle, A. Pesnelle (The Isolde Collaboration), and G. Huber, Nucl. Phys. **A367**, 1 (1981).
[53] L. E. Campbell and G. J. Perlow, Nucl. Phys. **A109**, 59 (1968).
[54] L. E. Campbell, G. L. Montet, and G. J. Perlow, Phys. Rev. B **15**, 3318 (1977).

[55] W. Thomas, K. Kroth, E. Bodenstedt, and J. Lange, Nucl. Phys. **A318**, 97 (1979).
[56] C. W. White, W. M. Hughes, G. S. Hayne, and H. G. Robinson, Phys. Rev. A **7**, 1178 (1973).
[57] Carol E. Tanner and Carl Wieman, Phys. Rev. A **38**, 1616 (1988).
[58] R. M. Sternheimer, Z. Naturforsch. **41a**, 24 (1986).
[59] M. S. Dewey, H. -E. Mahnke, P. Chowdhury, U. Garg, T. P. Sjoreen, and D. B. Fossan, Phys. Rev. C **18**, 2061 (1978).
[60] H. Kruger, O. Lutz, and H. Oehler, Phys. Lett. **A62**, 131 (1977).
[61] J. Bauche, J. -F. Wyart, Z. Ben Ahmed, and K. Guidara, Z. Phys. A **304**, 285 (1982).
[62] E. Gerdau, H. Winkler, and F. Sabathil, Hyperfine Interact. **4**, 630 (1978).
[63] W. Fischer, H. Huhnermann, and K. Mandrek, Z. Phys. **254**, 127 (1972).
[64] W. Borchers, E. Arnold, W. Neu, R. Neugart, K. Wendt, G. Ulm, and (ISOLDE Collaboration), Phys. Lett. **B216**, 7 (1989).
[65] W. Rijswijk, F. G. Berg, W. R. Joosten, and W. J. Huiskamp, Hyperfine Interact. **15**, 325 (1983).
[66] D. C. Palmer, A. D. Irving, P. D. Forsyth, I. Hall, D. G. E. Martin, and M. J. Maynard, J. Phys. G **4**, 1143 (1978).
[67] A. D. Irving, P. D. Forsyth, I. Hall, and D. G. E. Martin, J. Phys. G **5**, 1595 (1979).
[68] G. Marest, R. Haroutunian, I. Berkes, M. Meyer, M. Rots, J. De Raedt, H. Van de Voorde, H. Oonis, and R. Coussement, Phys. Rev. C **10**, 402 (1974).